Investigation on gas migration in saturated geo-materials with low permeability

L. XU [a], W. M. Y E[a,b,*], B. Ye[a], B. Chen [a], Y. G. Chen [a], Y. J. CUI [a,c]

a. Key Laboratory of Geotechnical and Underground Engineering of Ministry of Education, Tongji University, Shanghai 200092

b. United Research Center for Urban Environment and Sustainable Development, the Ministry of Education, Shanghai 200092

c. Ecole des Ponts ParisTech, UR Navier/CERMES, France，77455

Corresponding author

Prof. Weimin YE

Tel.: +86 21 6598 3729

Fax: +86 21 6598 2384

E-mail: ye_tju@tongji.edu.cn

Abstract: Investigation of the hydro-mechanical effects on gas migration in saturated materials with low permeability is of great theoretical and practical significances in many engineering fields. The conventional two-phase flow (visco-capillary flow) theory, which regards the capillary pressure as the only controlling factor in gas migration processes, is commonly adopted to describe the gas flow in geo-materials. However, for materials with low permeability, the conventional two-phase flow theory cannot properly describe the gas migration. In this work, hydro-mechanical coupled gas injection tests were conducted. The volumetric variation of the liquid for applying the confining pressure in the specimen cell and the gas flow rate were monitored. Test results indicate that gas migration was influenced by the capillary pressure and the mechanical stress simultaneously. The two key parameters of the gas entry pressure P_{entry} and the gas induced-dilatancy pressure $P_{dilatancy}$ are introduced for description of gas migration with respect to the capillary pressure and the mechanical stress effects, respectively. When the gas injection pressure is smaller than the P_{entry} and the $P_{dilatancy}$, the balance between the gas injection pressure and the confining pressure will lead to an intermittent gas flow. Sudden increase of gas flow rate could be observed once the gas injection pressure approaches the P_{entry} or the $P_{dilatancy}$. For higher gas injection pressures, the mechanical stress effects on gas migration could not be neglected. The sudden increase of gas flux under high gas injection pressures could be caused by the mechanical induced-dilatancy of channels, capillary pressure induced-continuous flow pathways, as well as the failure of sealing-efficiency. The failure of sealing-efficiency is closely related to the difference between the gas injection pressure and the confining pressure rather than the properties of the material tested. Monitoring the volume of liquid for applying confining pressure is helpful for detecting the failure of sealing efficiency and the mechanism of gas

breakthrough.

Keywords: gas migration; low permeability; gas entry pressure; gas induced-dilatancy pressure; the failure of sealing efficiency; gas breakthrough

1. Introduction

Problems related to gas migration in saturated materials with low permeability are widely encountered in engineering activities. For gas exploration, it is necessary to find out the gas permeability of geological formations for production planning, efficient exploration and resources management (Olatunji et al., 2015; Ahmadi et al., 2015). In the environmental remediation of contaminated sites using air-sparging technique, it is important to understand the gas flow capacity of the geo-materials in order to assess the remediation significance of the contaminated site (Chen et al., 2012). In CCS (CO_2 capture and storage) projects, understanding the permeability of supercritical CO_2 in porous rocks is of great significance in predicting the migration and evaluating the long-term stability of injected CO_2 (Javaheri et al., 2013; Ye et al., 2015). During the long-term operation of a deep geological repository for disposal of high-level nuclear waste, a great deal of gas will be produced by anaerobic corrosion of metals, radiolysis of water and microbial degradation of organic materials. Profound understanding of the mechanism of gas migration in buffer/backfill materials with ultra-low permeability is obligatory for safety assessment of the deep geological repository (Xu et al., 2013; Ye et al., 2014; Liu et al., 2015). Therefore, the determination of gas permeability of geo-materials, especially for those with low or ultra-low permeability, is of great theoretical and practical importance.

In this regards, the conventional two-phase flow (visco-capillary flow) theory, which regards the capillary pressure as the only controlling factor in gas migration processes, was commonly

adopted to describe the gas flow in geo-materials (Burdine, 1953; Brooks and Corey, 1964; Mualem, 1976; van Genuchten, 1980; Parker et al., 1987; Luckner et al., 1989; Adams et al., 1999; Ho et al., 2006; Kamiya et al., 2006). As described by the conventional two-phase flow theory, gas will entry the porous medium and directly displace the pore-water driven by the capillary pressure, which is defined as the difference between the gas-pressure and the liquid-pressure, leading to the de-saturation of the materials.

However, for materials with low permeabilities, the conventional two-phase flow theory could not properly describe the gas migration processes (Horseman et al., 1999; Marschall et al., 2005; Alonso et al., 2006). In low permeability materials, for low gas injection pressure, almost no gas outflow can be detected due to the significant boundary layer effects and the interfacial tension, while as the gas injection pressure increases to a relatively high (critical) value, a sudden increase of gas outflow might be recorded, which was widely termed as the gas breakthrough (Gallé, 2000; Wang, 2006; Popp et al., 2007; Yu et al., 2012; Song et al., 2015). This phenomenon could be explained using the gas entry pressure, P_{entry}, as shown in the water retention curve (Fig. 1) based on the conventional two-phase flow theory. For low gas injection pressure, the drainage of pore-water cannot happen due to the flow resisting force originated from the bound water film and the capillary effects. Consequently, almost no gas migration in the materials can be observed. However, when the gas injection pressure increased to a value about the gas entry pressure, a sudden gas flow could be detected due to the formation of continuous flow pathway in the materials (Wang, 2006; Hildenbrand et al., 2002). Clearly, all these explanations were based on the conventional two-phase flow theory, which regarded that the gas flow was only controlled by the capillary pressure.

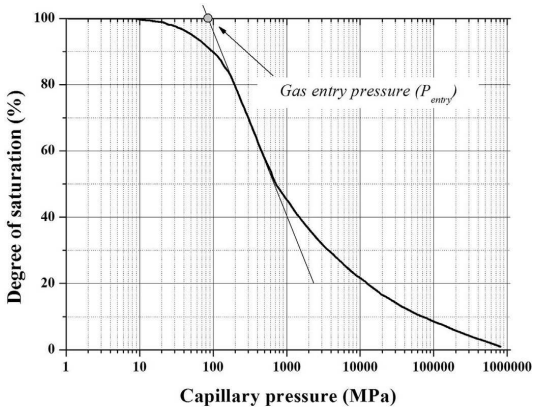

Fig. 1 Typical water retention curve in soils

In fact, except for the capillary pressure, the mechanical stress (i.e. the confining pressure, the pore fluid pressure) could be another important influencing factor to the gas flow in low permeability materials, especially, in an ultra-low permeability medium ($<10^{-20}m^2$) (Zhao, 2002; Marshall et al., 2005; Senger et al., 2008). This may be because that the extremely high threshold of capillary pressure for gas migration makes the conventional two-phase flow with drainage of pore-water is almost impossible, the significant gas flow only occurs in the dilatant pathways formed by the mechanical-stress (Popp et al., 2007; Yu et al., 2009 and Navarro, 2009). The critical pressure corresponding to the sudden increase of gas flow could be defined as the gas induced-dilatancy pressure, $P_{dilatancy}$. In this regard, lots of contributions have been made for investigation of influences of the mechanical stress on gas migration (Horseman et al., 1999; Marshall et al., 2005; Yu et al., 2009; Vardon et al., 2013; Ye et al., 2014). However, for almost all of these works, influence of the mechanical stress on gas migration was indirectly deduced from the measured variation of gas flow rate. In this way, it is difficult to distinguish the sudden increase of gas flow (gas breakthrough) is induced by the capillary pressure or the mechanical effects when the gas injection pressure approaches the value of P_{entry} or $P_{dilatancy}$. Horseman et al. (1999) once proposed that, for elaborately investigation of the mechanical effects on gas migration

processes, the analysis of volumetric behavior during gas migration was necessary.

At the same time, statistical results shown that for gas migration in ultra-low permeability materials, the gas breakthrough was only caused by the mechanical induced-dilatancy of flow pathways when the ratio of the gas injection pressure to the confining pressure was located in 0.7-1.1 (Horseman et al., 1999; Popp et al., 2007; Yu et al., 2009; Navarro, 2009). However, it should be noticed that, besides the possible dilatancy of the flow pathways, the failure of the sealing efficiency under such high gas injection pressure could also lead to significant gas outflow. Therefore, it is necessary to determine that the significantly increased gas flow rate of geo-materials with low permeability was caused by the dilatancy of the flow pathways or the failure of the sealing efficiency.

In this article, a series of step-by-step gas injection tests under constant confining pressures were conducted. The gas outflow rate and the liquid volume for applying the confining pressure in the specimen cell were carefully monitored during the whole tests. The volumetric variations of the specimen were calculated and the influences of the mechanical stress on gas migration processes were analyzed.

2. Experimental investigation

2.1 Test apparatus

The experimental setup for gas migration test is shown in Fig. 2. It is composed of six parts: a specimen cell for application of an isotropic confining pressure; two injection units (water injection unit and gas injection unit) for inlet/outlet of de-ionized water and high-purity Helium gas respectively; a volume/pressure controller for controlling the confining pressure and measuring the volumetric variation of liquid for applying confining pressure; a heating unit for

temperature control, a measurement system including a gas pressure transducers and three gas mass flowmeters (0.01-5 ml/min, 1-100 ml/min and 10-1000 ml/min at STP) for monitoring and recording the gas injection pressure and the gas outflow rate etc.

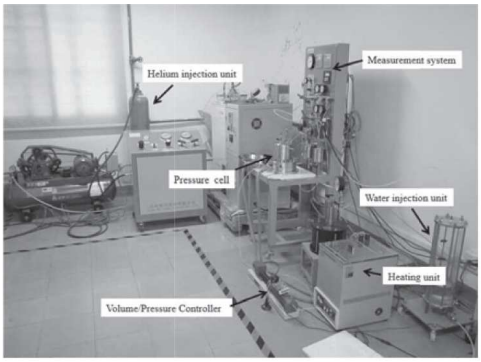

(a) Physical picture

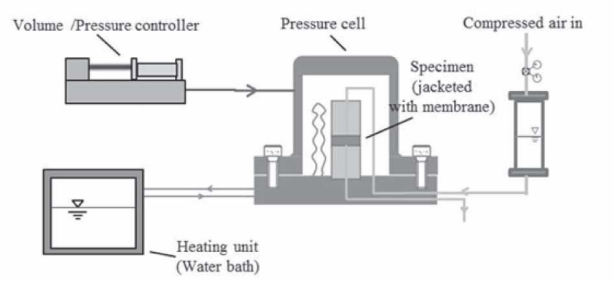

(b) Schematic diagram of water injection

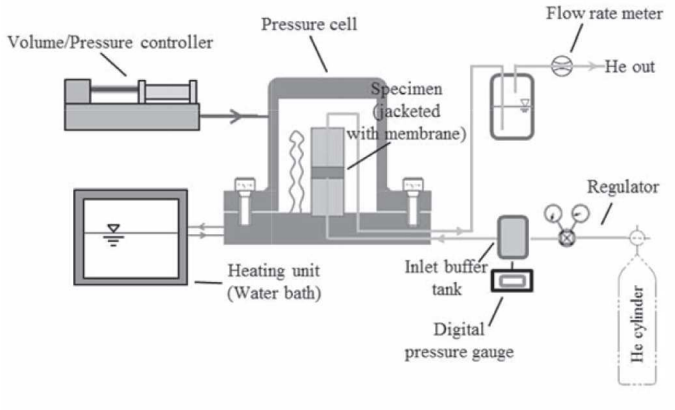

(c) Schematic diagram of gas injection

Fig. 2 Experimental apparatus for gas migration test

2.2 Materials and specimen preparation

Soft clay tested in this work was obtained from Pudong district of Shanghai, China. Some

basic physical properties and the cumulative particle size distribution curve of the soft clay are summarized in Tab. 1 and Fig. 3.

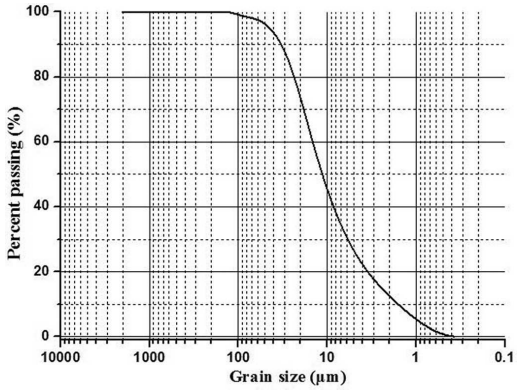

Fig. 3 Particle size distribution curve of the soft clay

Table 1 Basic physical properties of soft clay

Natural water content(%)	Specific gravity	Density(g/cm^3)	Void ratio	Liquid limit (%)	Plastic limit (%)	Plasticity index
42.35	2.73	1.797	1.16	42.0	21.5	20.5

For specimen preparation, after oven-dried at 60℃ for 72h, the intact specimen was ground into powder and sized through a 0.5 mm sieve. Then, the powder was statically compacted into target cylindrical specimens with a dimension of 10 mm in height, 50 mm in diameter and a designed dry density of 1.70 Mg/m^3.

2. 3 Test procedures

For investigation of the hydro-mechanical coupling effects on gas migration behavior, three step-by-step gas injection tests were conducted on the compacted specimens under confining pressures of 800kPa, 1100kPa and 1400kPa. Each test was fulfilled with the following stages.

1) Saturation and stress equilibrium

The apparatus used in this stage is shown in Fig. 2(b). After pushed out from the compaction

mould, the compacted specimen was sandwiched with two sintered stainless steel porous discs. Then, the sandwiched specimen was inserted into a Teflon heat-shrink tube and installed in the specimen cell. A target confining pressure was applied and kept constant during the whole test. After about 30 mins' stress equilibrium, water injection unit was connected and de-ionized water was injected (40kPa) from the upper end of the specimen (Fig. 2(b)). The water outflow and the volumetric variation of liquid in the specimen cell were monitored. This stage lasted for 7 to 10 days until the stable of the water outflow and the volumetric variation were reached.

2) Gas injection test

After the stage of saturation and stress equilibrium, connection of water injection unit was replaced by the gas injection unit (Fig. 2(c)). Then, high-purity Helium gas was initially injected with a gas pressure of 40kPa. The gas outflow rate and the volumetric variation of liquid in the specimen cell were monitored simultaneously. When the gas outflow rate and the liquid volumetric variation became steady, the gas injection pressure was increased by 50-100kPa. This procedure was repeated until the 'gas breakthrough' was observed.

New specimen was installed and the two steps mentioned above were repeated with the next confining pressure until all the three tests were conducted.

All the tests were conducted in an ambient temperature of 20±0.1℃.

3. Test results and analysis

3.1 Influence of mechanical stress on evolutions of gas flow rate

The gas injection pressure applied and the corresponding gas outflow rates measured with time under different confining pressures were presented in Fig. 4.

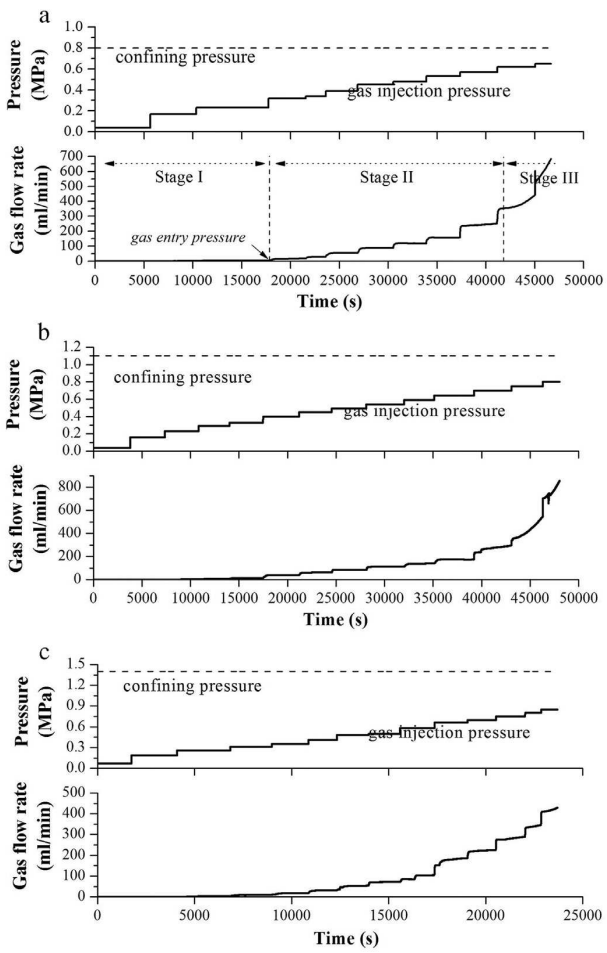

Fig. 4 Evolutions of gas flow rate with time under different confining pressures

Fig. 4(a) clearly shows that the evolution curve of gas migration with time can be divided into three distinctive stages.

In stage I, there was no significant gas flux from the specimen can be observed for the gas injection pressure lower than 200-300kPa, which almost equals to the gas entry pressure (P_{entry}) of the soil tested (Ye et al., 2008). This phenomenon could be explained using the conventional two-phase flow theory (Wang, 2006; Yu et al., 2012 and Song et al., 2015). Under relatively lower gas injection pressures, gas only exists in trapped and separated bubbles due to the significant boundary layer effects and the capillary effects in dense materials. Consequently, it is impossible to form continuous flow pathways and significant gas flux could not happen in this stage. However, based on test results on ultra-low permeability materials, Alkan et al. (2008) and Liu et

al. (2014) found that, although the continuous flow pathways were not formed due to the gas injection pressure lower than the P_{entry}, the intermittent and discontinuous flow was also observed, which may imply the mechanical stress influence on the gas flow.

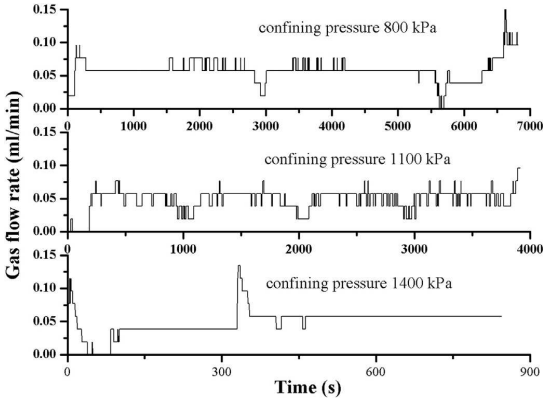

Fig. 5 Evolutions of gas flow rate with time for low gas injection pressures (<100kPa)

In this work, measured evolutions of gas flow rate with time in low gas injection pressures (below the P_{entry}) were presented in Fig. 5. Fig. 5 indicated that, although the gas injection pressure kept constant at low values, obvious fluctuations of gas flow rates were still recorded. These fluctuations could be induced by the intermittent opening and closing of pathways (Alkan et al. 2008; Harrington et al. 2012 and Liu et al. 2014). With the physical model shown in Fig. 6, it was suggested that, due to the low permeability of the material, the fluid pressure in the flow pathways (denoted as p in Fig. 6) will increase with the increase of the gas injection pressure. Once the fluid pressure in the flow pathways reached a threshold pressure (p_t) the flow pathways dilated with an increase of the flow pathways aperture (a), followed by a gas propagation, as well as the significant gas flux (q). After this, a relaxation period occurred, in which the fluid pressure and the gas flux dropped off, the pathway closed, and then the fluid pressure will be accumulated again. In this way, the flow pathways open and close episodically, resulted in fluctuation of gas flux during the gas migration process. Obviously, this stress-induced fluctuation could not be

explained only using the capillary pressure proposed by Wang, (2006), Yu et al., (2012) and Song et al., (2015).

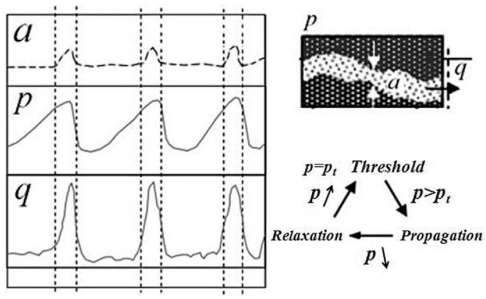

Fig. 6 The changes of pressure (p), flow rate (q) and pathway aperture (a) during the intermittent flow process (Alkan et al., 2008)

The second stage (II) of the gas flow rate curve presented in Fig. 4(a) indicated that, unlike that in the first stage, a steady-increasing gas flow rate could be observed once the gas injection pressure surpassed the P_{entry} of the soil tested. This phenomenon may imply that the conventional two-phase flow (capillary pressure controlled flow) was become more remarkable than that in the first stage. However, the mechanical stress could still influence the gas flow. With the increase of gas injection pressure, more stable and widen pathways were formed (Liu et al., 2014). Therefore, the gas flow rate increased stably with the driving forces of the capillary pressure and the mechanical stress simultaneously.

In the stage III in Fig. 4(a), an ever-increasing gas flow rate was observed as the gas injection pressure approached the confining pressure. Similar phenomena were also reported by other researchers as shown in Fig. 7, which was commonly recognized that it was resulted from a sudden dilatancy of the flow pathways under the high gas injection pressures (Horseman et al., 1999; Senger et al., 2008; Navarro, 2009 and Yu et al., 2009). However, with consideration of the test results during stage III in Fig. 4, it could be possible that the ever-increased gas flow rate was not only caused by the dilatancy of flow pathways but also caused by the failure of the sealing

efficiency of the flexible boundary.

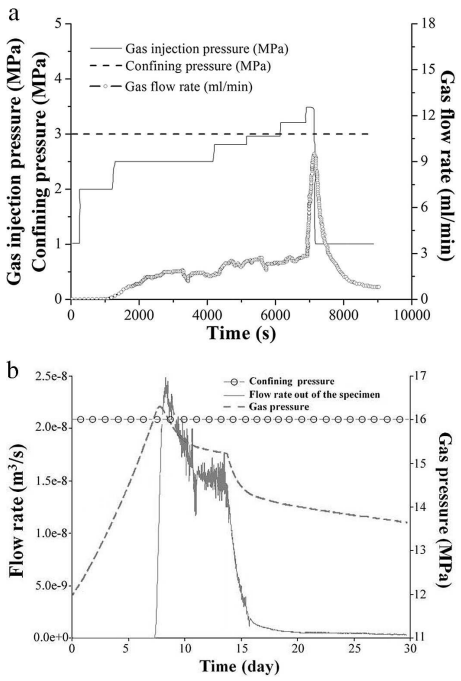

Fig. 7 Gas migration tests results in ultra-permeability materials

3.2 Influence of mechanical stress on volumetric deformation of the specimen

Measured volumetric variations of liquid in the specimen cell with gas injection pressure under different confining pressures were presented in Fig. 8.

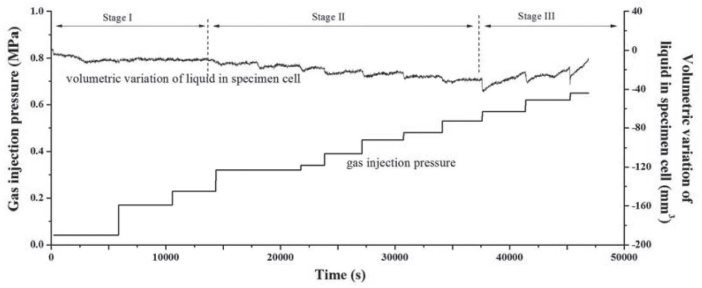

(a) Confining pressure 800kPa

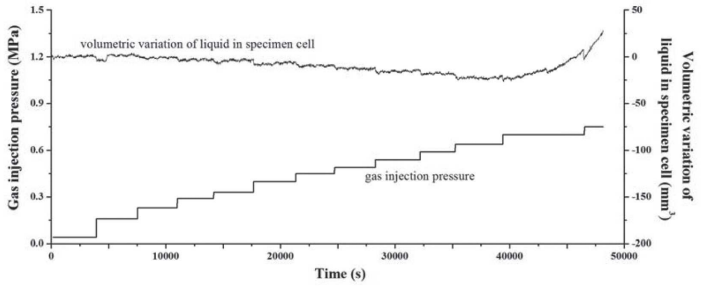

(b) Confining pressure 1100kPa

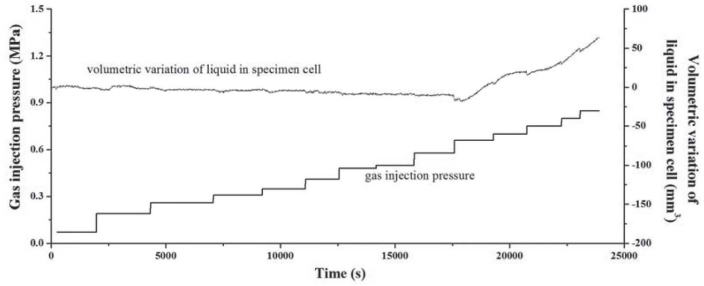

(c) Confining pressure 1400kPa

Fig. 8 Evolutions of volumetric variation of liquid in the specimen cell with time under different confining pressures

Fig. 8 shows that, as the gas injection pressure increases, the volumetric variation of liquid in the specimen cell slightly decreases, indicating a slight increase of specimen volume. Then, it turns to an accelerated abruptly increase, which indicates the liquid flow into the specimen cell significantly. In the meantime, amplitude of the measured volumetric variation of the confining liquid increases as the gas injection pressure increases. However, this phenomenon of fluctuation is faded with the increase of the confining pressure.

Similar to that of the gas flow rate curve shown in Fig. 4, the evolution curve of volumetric variation with gas injection pressure also can be divided into three stages (Fig. 8a).

In stage I (Fig. 8a), slight fluctuation of volumetric curve can be observed, which indicates the slight fluctuation of the volumetric deformation of the specimen. This observation may directly confirm that the fluctuations of gas flow rate (Fig. 5) were resulted from the periodically

opening and closing of the pathways induced by the balance between the gas injection pressure and the confining pressure.

During stage II, the measured volumetric variation stepwisely declined with increase of the gas injection pressure. Correspondingly, the volumetric deformation of the specimen increased with the increase of the gas injection pressure. This phenomenon may indicate that, with the increase of gas injection pressure, the size of flow pathways increases. With consideration of the variations of gas flow rates in Fig. 4, it can be concluded that gas flow in this stage was controlled both by the capillary pressure and the mechanical stress. This conclusion was confirmed by the test results of a Shanghai clay conducted by Wang (2006). Significant deviation can be observed between the calculated gas flow rate using the only conventional two-phase flow theory and the measured ones obtained by Wang (2006) in Fig. 9. Therefore, the mechanical stress effects could not be ignored for estimation of gas flow behaviors in this stage.

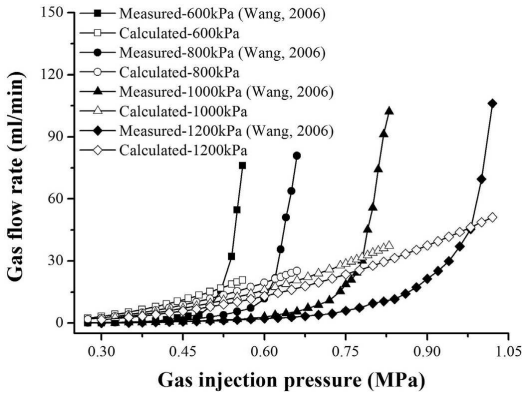

Fig. 9 Gas flow rates of specimens obtained under different vertical stresses

In stage III, the measured volumetric variation of the liquid in the specimen cell increased sharply with the increase of gas injection pressure (Fig. 8). This may indicates that the sudden “increase” of the measured volume of water into the specimen cell was caused by the failure of the sealing efficiency of the flexible boundary, which results in water flowing through the interface

between the specimen and the Teflon heat-shrink tube. This conclusion indicates that the measured volumetric variation of the liquid in the specimen cell in this stage could not reflect the volumetric variation of the specimen.

3.3. Determination of gas induced-dilatancy pressure $P_{dilatancy}$

Relationship between the effective stress (the difference between the confining pressure P_c and the gas injection pressure P_g) and the volumetric deformation of the specimen (deduced from the measured volumetric variation of the liquid in the specimen cell) at different confining pressures were fitted and plotted in Fig. 10.

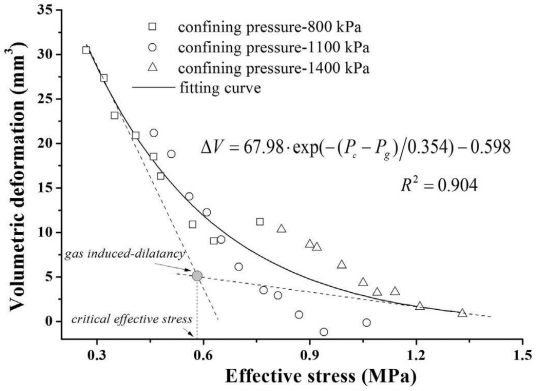

Fig. 10 Relationship between the effective stresses and the volumetric deformations of the specimens

Fig. 10 indicates that there is an exponential relationship between the volumetric deformation and the effective stress measured at different confining pressures. The volumetric deformation can be fitted,

$$\Delta V = 67.98 \cdot \exp(-(P_c - P_g)/0.354) - 0.598 \qquad R^2 = 0.904 \tag{1}$$

Here, ΔV is the volumetric deformation of the specimen; P_c is the confining pressure; P_g is the gas injection pressure.

In Fig. 10, the intersection point of two tangent lines of the fitted curve could be defined as

the “gas induced-dilatancy” of the material tested. The gas pressure corresponding to the threshold point was termed as gas induced-dilatancy pressure, $P_{dilatancy}$. When the gas injection pressure was applied higher than this threshold, gas migration may be mainly governed by mechanical stress, while for the gas injection pressure was lower than that value, the mechanical stress was not significant and gas flow may be mainly controlled by the capillary pressure.

4. Discussion

4.1 Mechanism of gas migration

According to the analyses in previous sections, gas migration processes in saturated low permeability materials were governed by both the capillary pressure and the mechanical stress.

The capillary pressure effects can be described by the conventional two-phase flow theory. The increase of the capillary pressure will overcome the flow resistance originated from the boundary effects and the interfacial tension, which results in the drainage of the pore-water. When the capillary pressure approaches the gas entry pressure (P_{entry}) of the materials, formation of the continuous gas flow pathways will results in significantly increasing of gas outflow. The gas entry pressure is closely related to the material properties, especially the size and shape of the flow pathways.

The increase of the gas injection pressure will lead to the intermittent open and close of pathways, follows by increases of pore-volumes and the final dilatancy of flow channels in the specimen. According to Fig. 10, the mechanical stress effects on the gas migration process was limited for low gas pressures, while when the gas injection pressure increases to the gas induced-dilatancy pressure ($P_{dilatancy}$), the stress state effects may become significant and results in a remarked gas flux.

Therefore, P_{entry} and $P_{dilatancy}$ are two important parameters for description of the capillary pressure and mechanical stress effects on gas flow. The relationship between the P_{entry} and the $P_{dilatancy}$ depended on the material properties and stress state simultaneously.

Based on the test results in this work and the definition of $P_{dilatancy}$ given in Fig. 10, the gas entry pressure and gas induced-dilatancy pressure were listed in Table. 2.

Table. 2 The critical pressures presented in gas injection tests

Confining pressure P_c (kPa)	Gas entry pressure P_{entry} (kPa)	Critical effective stress* (kPa)	Gas induced-dilatancy pressure $P_{dilatancy}$ (kPa)	$P_{dilatancy}$ /P_{entry}
800	231	575	225	0.974
1100	280		525	1.875
1400	310		825	2.661

* The critical effective stress was defined as the effective stress corresponding to the gas induced-dilatancy indicated in Fig. 10.

In Tab. 2, the ratio of $P_{dilatancy}/P_{entry}$ decreased with decrease of the confining pressure. This phenomenon indicated that for a lower confining pressure, the $P_{dilatancy}$ could be equal to or lower than the P_{entry}. For example, for specimen tested at a confining pressure of 800kPa, the gas induced-dilatancy pressure (225kPa) was lower than its gas entry pressure (231kPa). The relationship between the $P_{dilatancy}$ and the P_{entry} will depend on the material properties and the stress states. Therefore, for materials with relatively higher permeability, the gas entry pressure was relatively low. For a sufficient confining pressure, the P_{entry} is generally lower than $P_{dilatancy.}$

and the gas flow curve could be divided into three stages.

For extremely dense material with relatively lower confining pressures, the value of $P_{dilatancy}$ may be much smaller than that of P_{entry} and the gas flow will be only governed by the mechanical stress (Horseman et al., 1999; Ye et al., 2014). In this case, the stage between the P_{entry} and the $P_{dilatancy}$ will disappear and only two stages of gas flow can be identified (Fig. 7b).

4.2 Gas breakthrough

The gas induced-dilatancy pressure ($P_{dilatancy}$) had been widely investigated and its value was determined through the measured variation of gas flow rate (Horseman et al., 1999; Yu et al., 2009). Common recognition reached that the value of $P_{dilatancy}$ was closely related to that of the confining pressures (P_c) (Tab. 3).

Table. 3 Gas induced-dilatancy pressure and confining pressure

Confining pressure P_c (MPa)	Gas induced-dilatancy pressure $P_{dilatancy}$ (MPa)	$P_{dilatancy}$ /P_c	Soil	References
16	15.93	0.99	MX80-high swelling	Horseman et al. (1999)
18	16.38	0.91	MX80-high swelling	Horseman et al. (1999)
20	18.02	0.90	MX80-high swelling	Horseman et al. (1999)
22	18.92	0.86	MX80-high swelling	Horseman et al. (1999)

8	7.85	0.98	MX80-medium swelling	Horseman et al. (1999)
9	8.90	0.99	MX80-medium swelling	Horseman et al. (1999)
3	3.2	1.07	Opalinus clay	Popp et al. (2007)
14-15	10-12	0.70-0.86	Host rock in Benken borehole	Navarro (2009)

In Tab. 3, the ratio of the gas induced-dilatancy pressure to the confining pressure for different soils tested is mainly located in 0.7-1.1. Therefore, common conclusions can be reached that gas induced-dilatancy occurred when the gas injection pressure approached or surpassed the confining pressure (Horseman et al. 1999; Popp et al. 2007). In this regard, the ratio of the $P_{dilatancy}$ to the P_c was widely adopted for establishing theoretical models for simulation of gas migration in low permeability materials (Eqs. (2) and (3)). Regarded that $P_{dilatancy}$ equals to 0.76 P_c, Navarro (2009) once proposed,

$$k_{\text{dilatancy}}(P_g)=\begin{cases}0 & for P_g \le P_{dilatancy}\\ \left(\dfrac{P_g - P_{dilatancy}}{\Delta P}\right)^{a_1}\Delta k_{\text{dilatancy}} & for P_g > P_{\text{dilatancy}}\end{cases} \tag{2}$$

$$k_{\text{int}} = f(P_g)k_{\text{int}}^{ini}=\begin{cases}(1+a_2P_g)k_{\text{int}}^{ini} & for P_g \le P_{dilatancy}\\ (a_3(P_g - P_{\text{dilatancy}})+1+a_2P_{\text{dilatancy}})k_{\text{int}}^{ini} & for P_g > P_{\text{dilatancy}}\end{cases} \tag{3}$$

Where, $k_{\text{dilatancy}}$ is the gas pressure-dependent permeability; ΔP is the pressure interval over which gas permeability changes by $\Delta k_{\text{dilatancy}}$, $P_{\text{dilatancy}}$ is the critical value denoted as the gas induced-dilatancy pressure, k_{int} and k_{int}^{ini} are the intrinsic permeability and initial intrinsic permeability respectively; a_1, a_2 and a_3 are parameters to be fitted.

However, it should be noted that the determination of the gas induced-dilatancy in an indirect way through the sudden increase of gas flow rates is open to discussion. Based on the measured relationship between the gas flow rate and the injection pressure in the low-permeability materials of Opalinus Clay and MX80-bentonite, Popp et al. (2007) and Horseman et al. (1999) concluded that the sudden increase of gas flux was caused by the mechanical induced-dilatancy of channels rather than the capillary pressure evoked-formation of continuous pathway due to the extremely high gas entry pressure of the materials tested. However, as another reason, the failure of sealing efficiency could not be neglected, especially when the ratio of injection pressure to the confining pressure reached 0.7~1.1. For the measured evolution of gas flow rate of Shanghai soft clay with relatively lower gas-entry pressure in Fig. 4, sudden increase of gas flux could be caused by the mechanical induced-dilatancy, as well as the capillary pressure induced-continuous flow pathways. However, the possibility of the failure of sealing efficiency under a high ratio of the gas injection pressure to the confining pressure around 0.7 can be confirmed based on analysis of the measured volumetric variation of liquid used for applying confining pressure in Fig. 8. In Fig. 8, the sudden “increase” of the measured volume of liquid in the specimen cell indicated that water flow through the interface between the specimen and the Teflon heat-shrink tube.

Therefore, the sudden increase of gas flux under high gas pressure could be caused by the mechanical induced-dilatancy of channels, capillary pressure induced-continuous flow pathways, as well as the failure of sealing-efficiency. The failure of sealing-efficiency was closely related to the difference between the gas injection and the confining pressures rather than the properties of the material tested. Monitoring the volume of liquid for applying confining pressure can help for detection the failure of sealing efficiency and investigation the mechanism of gas breakthrough.

5. Conclusions

In this study, stepwise gas injection tests were conducted on remolded Shanghai clay under different confining pressures. The gas flow rates and the volume of liquid for applying the confining pressure were simultaneously monitored. Results were analyzed and some conclusions were obtained.

The capillary pressure and the mechanical stress both played important roles during the gas migration process. The capillary pressure effects can be described by the conventional two-phase flow theory, while the mechanical stress influences can be described by an exponential relationship between the volumetric deformation of the specimen and the effective stress. The parameters P_{entry} and the $P_{dilatancy}$ could be employed for description of the capillary pressure and the mechanical stress effects, respectively.

The relationship between the P_{entry} and the $P_{dilatancy}$ depended on the material properties and the stress states. Based on this, gas migration process could be divided into two- or three- stages according to the relationship between the P_{entry} and the $P_{dilatancy}$. For the gas injection pressure lower than the P_{entry} and the $P_{dilatancy}$, an intermittent gas flow rate could be observed due to the balance between the gas injection pressure and the confining pressure. Significant gas flow rate could be observed once the gas pressure reaches the P_{entry} or the $P_{dilatancy}$. For higher gas injection pressures, the mechanical stress effects on gas migration could not be neglected.

Sudden increase of gas flux under high gas injection pressures (gas breakthrough) could be caused by the mechanical induced-dilatancy of channels, capillary pressure induced-continuous flow pathways, as well as the failure of sealing-efficiency. The failure of sealing-efficiency is closely related to the difference between the gas injection pressure and the confining pressure

rather than the properties of the material tested. For determination of the failure of sealing-efficiency and the mechanism of gas breakthrough, monitoring the volumetric variation of the liquid for applying the confining pressure, could be adopted.

Acknowledgements

The authors are grateful to the National High Technology Research and Development Program of China (863 Program: 2011AA050604, the National Natural Science Foundation of China (Projects No. 41030748), China Atomic Energy Authority (Project [2011]1051) for their financial support.

References

Adams, J.A., Reddy, K.R., 1999. Laboratory study of air sparging of TCE-contaminated saturated soils and ground water. Ground. Water. Monit. Rem. 19, 182–190.

Ahmadi, M.A., 2015. Connectionist approach estimates gas-oil relative permeability in petroleum reservoirs: Application to reservoir simulation. Fuel. 140, 429-439.

Alkan, H., Müller, W., 2008. Approaches for modelling gas flow in clay formations as repository systems. Phys. Chem. Earth. 33, 260-268.

Alonso, E.E., Olivella, S., Arnedo, D., 2006. Mechanisms of gas transport in clay barriers. J. Iber. Geol. 32(2), 175-196.

Brooks, R.H., Corey, A.T., 1964. Hydraulic Properties of Porous Media. Hydrology Paper No. 3, Fort Collins, CO, Colorado State University.

Burdine, N.T., 1953. Relative permeability calculations from pore size distribution data.

Transactions of the American Institute of Mining and Metallurgical Engineers. 198, pp. 71–78.

Chen, Y.G., Ye, W.M., Xie, Z.J., Chen, B., Cui, Y.J., 2012. Remediation of saturated Shanghai sandy silt contaminated with p-xylene using air sparging. Nat Hazards. 62, 1005-1020.

Gallé, C., 2000. Gas breakthrough pressure in compacted Fo-Ca clay and interfacial gas overpressure in waste disposal context. Appl. Clay. Sci. 17, 85-97.

Harrington, J.F., La Vaissière, R., Noy, D.J., Cuss, R.J., Talandier, J., 2012. Gas flow in Callovo-Oxfordian claystone (COx): results from laboratory and field-scale measurements. Mineral. Mag. 76(8), 3303-3318.

Hildenbrand, A., Schlomer, S., Krooss, B.M., 2002. Gas breakthrough experiments on fine-grained sedimentary rocks. Geofluids. 2-23.

Ho, C.K., Webb, S.W., 2006. Gas transport in porous media. Theory and Applications of Transport in Porous Media. Jacob, B. Technion- Israel Institute of Technology, Haifa, Israel Volume (20).

Hoseman, S.T., Harrington, J.F., Sellin, P., 1999. Gas migration in clay barriers. Eng. Geol. 54, 139-149.

Javaheri, M., Nattwongasem, D., Jessen, K., 2013. Relative permeability and non-wetting phase plume migration in vertical counter-current flow settings. Int. J. Greenhouse Gas Control. 12, 168-180.

Kamiya, K., Bakrie, R., and Honjo, Y., 2006. A New Method for the Measurement of Air Permeability Coefficient of Unsaturated Soil. Unsaturated Soils 2006. 1741-1752.

Liu, J. F., Davy, C.A., Talandier, J., Skoczylas, F., 2014. Effect of gas pressure on the sealing

efficiency of compacted bentonite-sand plugs. J. Contam. Hydrol. 170, 10-27.

Liu J. F., Skoczylas F., and Talandier J., 2015. Gas permeability of a compacted bentonite–sand mixture: coupled effects of water content, dry density, and confining pressure. Can. Geotech. J. 52, 1–9.

Luckner, L., van Genuchten, M.Th., Nielsen, D.R., 1989. A Consistent Set of Parametric Modelsfor the Two-Phase Flow of Immiscible Fluids in the Subsurface. Water. Resour. Res. 25(10), 2187–2193.

Marschall, P., Horseman, S., Gimmi, T., 2005. Characterization of gas transport properties of the Opalinus Clay, a potential host rock formation for radioactive waste disposal. Oil Gas Sci. Technol. –Rev. IFP 60 (1),121-139.

Mualem, Y., 1976. A New Model for Predicting the Hydraulic Conductivity of Unsaturated PorousMedia. Water. Resour. Res. 12(3), 513–522.

Navarro, M., 2009. Performance assessment methodologies in application to guide the development of the safety case (PAMINA). Simulating the migration of repository gases through argillaceous rock by implementing the mechanism of pathway dilation code TOUGH2. European Commission (Contract Number: FP6-036404).

Olatunji, S.O., Selamat, A., Azeez, A.E.A., 2015. Modeling permeability and PVT properties of oil and gas reservoir using hybrid model based type-2 fuzzy logic systems. Neurocomputing. 157, 125-142.

Parker, J.C., Lenhard, R.J., Kuppusamy, T., 1987. A Parametric Model for Constitutive Properties Governing Multiphase Flow in Porous Media. Water. Resour. Res. 23(4), 618–624.

Popp, T., Wiedemann, M., Böhnel, H., Minkley, W., 2007. Untersuchungen zur Barriereintegrität

im Hinblick auf das Ein-Endlager-Konzept. InstitutfürGebirgsmechanik GmbH, Leipzig, Germany.

Senger, R., Marschall. P., Finsterle, S., 2008. Investigation of two-phase flow phenomena associated with corrosion in an SF/HLW repository in Opalinus Clay, Switzerland. Phy. Chem. Earth 33, 317-326.

Song, H.Q., Cao, Y., Yu, M.X., Wang, Y.H., Killough, J.E., Leung, J., 2015. Impact of permeability heterogeneity on production characteristics in water-bearing tight gas reservoirs with threshold pressure gradient. J. Nat. Gas. Sci. Eng. 22, 172-181.

van Genuchten, M. Th., 1980. A closed-form equation for predicting the hydraulic conductivity of unsaturated soils. Soils. Sci. Soc. Am. J. 44, 892-898.

Vardon, P.J., Thomas, H.R., Masum, S.A., Chen, Q., Nicholson, D., 2013. Simulation of repository gas migration in a bentonite buffer. Engineering and Computational Mechanics. Special Issue Nuclear, 167 (EM1), 13-22.

Wang, C.S., 2006. The research on the permeating behavior of gas flow in saturated clay and its applying. Postdoctoral Report. Shanghai. Tongji University. (in Chinese)

Xu,W.J., Shao, H., Hesser, J.,Wang,W., Schuster, K., Kolditz, O., 2013. Coupled multiphase flow and elasto-plastic modelling of in-situ gas injection experiments in saturated claystone (Mont Terri Rock Laboratory). Eng. Geol. 157, 55–68

Ye, B., Ye, W.M., Zhang, F., Xu, L., 2015. A new device for measuring the supercritical CO_2 permeability in porous rocks under reservoir conditions. Geotech. Test. J. 38(3), 1-8.

Ye, W.M., Xu, L., Chen, B., Chen, Y.G., Ye, B., Cui, Y.J., 2014. An approach based on two-phase flow phenomenon for modeling gas migration in saturated compacted bentonite. Eng. Geol.

169, 124-132.

Ye, W.M., Wang, Q., Chen, B., Huang, Y., 2008. Advances in research on unsaturated characeristics of shanghai soft soil. Journal of Engineering Geology. 16(Suppl). 590-596. (in Chinese)

Yu, L., Weetjens, E., 2009. Summary of gas generation and migration. (SCK.CEN-ER-106.09/L Yu/P-85).

Yu, R. Z., Bian, Y.N., Li, Y., Zhang, X.W., Yan, J., Wang, H.C., Wang, K.J., 2012. Non-Darcy flow numerical simulation of XPJ low permeability reservoir. J. Petrol. Sci. Eng. 92-93, 40-47.

Zhao, Y.S., Hu, Y.Q., Zhao, B.H., Yang, D., 2002. Nonlinear coupled mathematical model for solid deformation and gas seepage in fractured media. Transport. Porous. Med. 53(2), 119-136.